

# Adaptive evolution to the natural and anthropogenic environment in a global invasive crop pest, the cotton bollworm

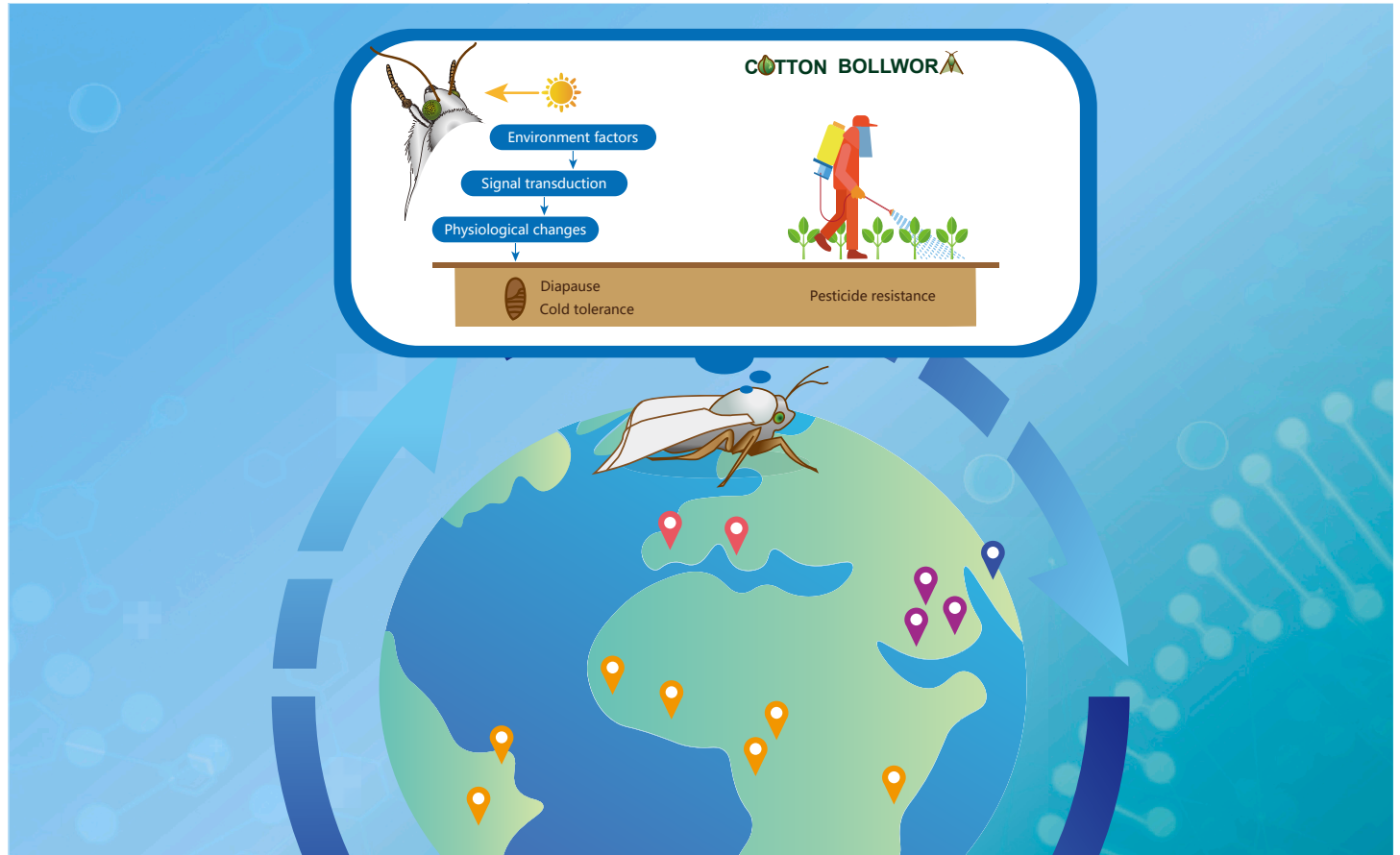
Minghui Jin,<sup>1,2,12</sup> Henry L. North,<sup>3,12</sup> Yan Peng,<sup>1,4,12</sup> Hangwei Liu,<sup>1,12</sup> Bo Liu,<sup>1,12</sup> Ruiqing Pan,<sup>6,12</sup> Yan Zhou,<sup>2,12</sup> Weigang Zheng,<sup>1</sup> Kaiyu Liu,<sup>7</sup> Bo Yang,<sup>1</sup> Lei Zhang,<sup>1</sup> Qi Xu,<sup>1</sup> Samia Elfekih,<sup>8,9</sup> Wendy A. Valencia-Montoya,<sup>10</sup> Tom Walsh,<sup>11</sup> Peng Cui,<sup>1</sup> Yongfeng Zhou,<sup>1</sup> Kenneth Wilson,<sup>1,5</sup> Chris Jiggins,<sup>3,\*</sup> Kongming Wu,<sup>2,\*</sup> and Yutao Xiao<sup>1,\*</sup>

\*Correspondence: [cj107@cam.ac.uk](mailto:cj107@cam.ac.uk) (C.J.); [wukongming@caas.cn](mailto:wukongming@caas.cn) (K.W.); [xiaoyutao@caas.cn](mailto:xiaoyutao@caas.cn) (Y.X.)

Received: February 14, 2023; Accepted: May 27, 2023; Published Online: May 30, 2023; <https://doi.org/10.1016/j.xinn.2023.100454>

© 2023 The Author(s). This is an open access article under the CC BY-NC-ND license (<http://creativecommons.org/licenses/by-nc-nd/4.0/>).

## GRAPHICAL ABSTRACT



## PUBLIC SUMMARY

- Population genomics reveals global population connectivity in the cotton bollworm.
- Adaptation in highly connected populations of a major agricultural pest.
- Genetic variation enables evolution of cold tolerance in the cotton bollworm.
- Climate and human activity shape evolution of the global crop pest *Helicoverpa armigera*.



# Adaptive evolution to the natural and anthropogenic environment in a global invasive crop pest, the cotton bollworm

Minghui Jin,<sup>1,2,12</sup> Henry L. North,<sup>3,12</sup> Yan Peng,<sup>1,4,12</sup> Hangwei Liu,<sup>1,12</sup> Bo Liu,<sup>1,12</sup> Ruiqing Pan,<sup>6,12</sup> Yan Zhou,<sup>2,12</sup> Weigang Zheng,<sup>1</sup> Kaiyu Liu,<sup>7</sup> Bo Yang,<sup>1</sup> Lei Zhang,<sup>1</sup> Qi Xu,<sup>1</sup> Samia Elfekih,<sup>8,9</sup> Wendy A. Valencia-Montoya,<sup>10</sup> Tom Walsh,<sup>11</sup> Peng Cui,<sup>1</sup> Yongfeng Zhou,<sup>1</sup> Kenneth Wilson,<sup>1,5</sup> Chris Jiggins,<sup>3,\*</sup> Kongming Wu,<sup>2,\*</sup> and Yutao Xiao<sup>1,\*</sup>

<sup>1</sup>Shenzhen Branch, Guangdong Laboratory of Lingnan Modern Agriculture, Key Laboratory of Gene Editing Technologies (Hainan), Ministry of Agriculture and Rural Affairs, Agricultural Genomics Institute at Shenzhen, Chinese Academy of Agricultural Sciences, Shenzhen 518116, China

<sup>2</sup>The State Key Laboratory for Biology of Plant Disease and Insect Pests, Institute of Plant Protection, Chinese Academy of Agricultural Sciences, West Yuanmingyuan Road, Beijing 100193, China

<sup>3</sup>Department of Zoology, University of Cambridge, Cambridge CB2 1SZ, UK

<sup>4</sup>College of Plant Science and Technology, Huazhong Agricultural University, Wuhan 430070, China

<sup>5</sup>Lancaster Environment Centre, Lancaster University, Lancaster LA1 4YW, UK

<sup>6</sup>Berry Genomics Corporation, Beijing 102200, China

<sup>7</sup>Institute of Entomology, School of Life Sciences, Central China Normal University, Wuhan 430079, China

<sup>8</sup>Australian Centre for Disease Preparedness (ACDP), CSIRO Health & Biosecurity, East Geelong, VIC 3169, Australia

<sup>9</sup>Bio21 Institute and the School of Biosciences, The University of Melbourne, Melbourne, VIC 3010, Australia

<sup>10</sup>Department of Organismic and Evolutionary Biology and Museum of Comparative Zoology, Harvard University, Cambridge, MA 02138, USA

<sup>11</sup>CSIRO Land and Water, Black Mountain Laboratories, Canberra, ACT 2601, Australia

<sup>12</sup>These authors contributed equally

\*Correspondence: [cj107@cam.ac.uk](mailto:cj107@cam.ac.uk) (C.J.); [wukongming@caas.cn](mailto:wukongming@caas.cn) (K.W.); [xiaoyutao@caas.cn](mailto:xiaoyutao@caas.cn) (Y.X.)

Received: February 14, 2023; Accepted: May 27, 2023; Published Online: May 30, 2023; <https://doi.org/10.1016/j.xinn.2023.100454>

© 2023 The Author(s). This is an open access article under the CC BY-NC-ND license (<http://creativecommons.org/licenses/by-nc-nd/4.0/>).

Citation: Jin M., North H.L., Peng Y., et al., (2023). Adaptive evolution to the natural and anthropogenic environment in a global invasive crop pest, the cotton bollworm. *The Innovation* 4(4), 100454.

The cotton bollworm, *Helicoverpa armigera*, is set to become the most economically devastating crop pest in the world, threatening food security and biosafety as its range expands across the globe. Key to understanding the eco-evolutionary dynamics of *H. armigera*, and thus its management, is an understanding of population connectivity and the adaptations that allow the pest to establish in unique environments. We assembled a chromosome-scale reference genome and re-sequenced 503 individuals spanning the species range to delineate global patterns of connectivity, uncovering a previously cryptic population structure. Using a genome-wide association study (GWAS) and cell line expression of major effect loci, we show that adaptive changes in a temperature- and light-sensitive developmental pathway enable facultative diapause and that adaptation of trehalose synthesis and transport underlies cold tolerance in extreme environments. Incorporating extensive pesticide resistance monitoring, we also characterize a suite of novel pesticide and Bt resistance alleles under selection in East China. These findings offer avenues for more effective management strategies and provide insight into how insects adapt to variable climatic conditions and newly colonized environments.

## INTRODUCTION

Invasive species are a threat to global biosafety, food security, and human health.<sup>1,2</sup> Traits that increase invasiveness, such as pesticide resistance or cold tolerance, often evolve under strong selection in novel environments.<sup>3</sup> Population genomics is a valuable tool for understanding the evolution and genetic basis of adaptations,<sup>4–7</sup> and it is now being used to study invasive pests. By identifying the genetic basis of rapidly arising adaptations that enable population expansion using population genomics approaches, the mechanisms of invasive spread can be revealed. Management strategies can then be developed and improved. The large effective population size and high connectivity of invasive species may explain the speed at which range-expanding adaptations are fixed. An example of this is the bridgehead effect.<sup>8</sup> Therefore, characterizing major routes of gene flow is important for managing and mitigating the effect of invasive species.<sup>9</sup>

The cotton bollworm, *Helicoverpa armigera* (Lepidoptera: Noctuidae), is a widespread crop pest in Afro-Eurasia and Australia, and it has recently become established in South America. Invasive *H. armigera* populations threaten to spread into North America by northward dispersal and through introgression with native sister species of *H. armigera*, *Helicoverpa zea*.<sup>10,11</sup> *H. armigera* is polyphagous, and the larvae feed on more than 180 plant species, including cotton, maize, soy, wheat, and rice.<sup>12</sup> *H. armigera* can undergo facultative pupal diapause to overwinter in non-tropical regions and avoid unfavorable winter conditions.<sup>13</sup>

Extensive use of synthetic pesticides has resulted in broad pesticide resistance in this species. *H. armigera* accounts for more reported cases of pesticide resistance than any other noctuid species.<sup>12,14</sup> A key tactic for cotton bollworm management currently involves cultivation of Bt crops. However, Bt resistance has been reported, especially in Asia and Australasia.<sup>15,16</sup> *H. armigera* has remarkable dispersal ability, and adults are capable of high-altitude, long-range flight.<sup>11</sup> Therefore, despite its extensive geographic range, little population structure has been observed using genetic markers, apart from the Australasian subspecies *H. armigera conferta*. This has made it difficult to characterize connectivity, identify locally adapted populations, and determine the source(s) of the invasive South American population.<sup>17,18</sup> *H. armigera* has readily spread through different environments from tropical plantations to dry, temperate, seasonal agroecosystems. Despite apparent panmixia, traits enabling *H. armigera* persistence, such as cold tolerance and diapause, known to have a genetic basis in *H. armigera*, show local adaptation in strains from high-versus low-latitude populations.<sup>19,20</sup> Therefore, delineating cryptic population differentiation and identifying local adaptation are important for determining the ecological and evolutionary factors that underlie regional *H. armigera* outbreaks. In other systems, the contiguity of resolution offered by population-scale whole-genome resequencing has been useful for resolving cryptic population structure and clarifying the genetic basis of traits under selection.<sup>4,5</sup>

*H. armigera* populations in China provide an ideal case study; its four highly distinct agricultural regions span climatic extremes and agricultural practices, separated by bio-geographic breaks of varying strength (Note S1). Collectively the largest agricultural industry in the world,<sup>21</sup> extensive wheat, cotton, and maize plantations in all four regions provide key habitats for the cotton bollworm. We generated a chromosome-scale reference assembly and produced a large whole-genome resequencing dataset of *H. armigera* individuals from samples throughout its global distribution, with a specific focus on Chinese populations, to characterize global population structure and identify local adaptation to anthropogenic and abiotic conditions.

## RESULTS

### Genomic diversity and population differentiation

We generated a chromosome-level assembly of the *H. armigera* genome with a size of 355.2 Mb and scaffold N50 of 12.74 Mb, using a combination of Oxford Nanopore Technologies (ONT) long reads and Illumina reads. This had a higher degree of contiguity, completeness, and accuracy than the *H. armigera conferta* genome (Figure S1; Tables S1–S3; Note S2).<sup>22</sup> A total of 18,455 coding genes were predicted, containing more than 96.6% of core-eukaryotic single-copy orthologs identified through BUSCO analysis (Figure S1B).

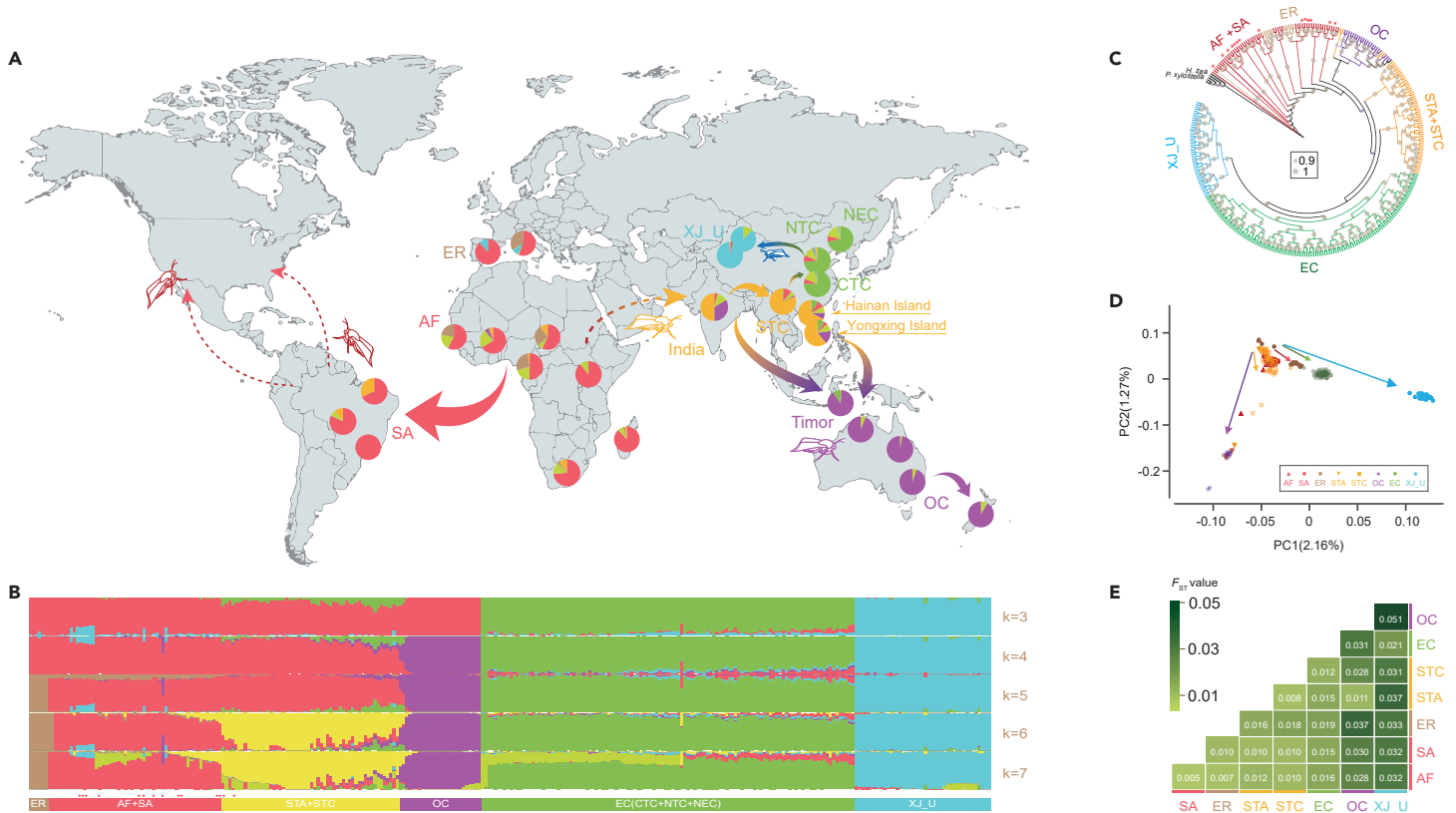


**Figure 1. Genome assembly and population structure** (A) Geographic distribution of 503 *H. armigera* samples. The colors of the pies represent ancestral components (according to the substructure at  $K = 7$ ). Putative spread routes of *H. armigera* are represented by arrows. (B) ADMIXTURE analysis for  $K = 3-7$ . Six subgroups are labeled: Europe (ER), Africa (AF), South America (SA), South Asia (STA), South China (STC), Oceania (OC), East China (EC), Central China (CTC), North China (NTC), Northeast China (NEC), and Xinjiang Autonomous Region (Xinjiang [XJ]). (C) A maximum-likelihood (ML) phylogenetic tree with two *Plutella xylostella* individuals and three *H. zea* individuals was used as an outgroup. Bootstraps are shown in gray circles. (D) PCA plots of the first two components and indicated paths of diffusion of *H. armigera* based on geographic origin. (E) Pairwise comparisons of fixation index ( $F_{ST}$ ) and diversity ( $\pi$ ) values between subgroups of *H. armigera*.

We obtained whole-genome sequence data of  $\sim 15.4\times$  coverage of 479 individuals, including 48 sample sites spanning almost all suitable areas for *H. armigera* worldwide, supplemented by public data of 24 individuals from multiple countries (Figure 1A; Tables S4–S6).<sup>23</sup> We mapped  $\sim 4$  Tb of raw sequence data from all individuals to our reference genome and called 1,051,382 high-quality SNPs for further analysis. We used multiple approaches to quantify the relatedness and population structure among these samples. ADMIXTURE analysis revealed a distinct population structure. The major groups identified with  $K = 3$  were (1) all of Afro-Eurasia and Oceania, (2) East China, and (3) the Xinjiang Uygur autonomous region (“Xinjiang” hereafter) (Figure 1B). A  $K$  value of 4 separated individuals sampled in Oceania within the first group, and  $K = 7$  further delineated European samples, African plus introduced South American samples, and South Asian plus South China samples.

Phylogenetic analyses revealed that samples from Africa and South America were the earliest diverging lineages and that samples from East China and Xinjiang indicated the formation of distinct clades (Figures 1C and S2A). Consistent with ADMIXTURE results, principal component 1 separated the three major lineages, and principal component 2 separated individuals sampled in Oceania (Figure 1D). To verify whether the sequencing depth between continents has an effect on population structure, we incorporated genotype probabilities analysis using PCAnsd and found that the results were consistent (Figure S2B). Although the variation in mean depth between continents showed no effect on population structure, increased individual sampling in unsampled regions of Africa and India could yield finer-scale population structure influenced by geography. The data analysis of population structure using the fixation index  $F_{ST}$  was consistent with this pattern despite globally low genetic differentiation (Figure 1E).

Population structure within China reflects the geographic barriers to gene flow (Figure 1B). Consistent with the geographic isolation of this region by deserts and mountains, the monophyletic Xinjiang lineage shows a highly distinct demographic history (Figure S3 and Note S3) and relatively low gene flow with populations in East China and South China (Figure 1E). Principal-component analysis

(PCA) and phylogenetic reconstruction showed that individuals sampled during northward and southward seasonal migrations across the Bohai Strait between Northeast and Central China clustered with the East China lineage (Figure S4; Note S3). This observation confirms that the cotton bollworm readily disperses over large distances across Central, Northern, and Eastern China. In contrast, individuals from South Asia clustered with the South China clade, suggesting high connectivity between South China and other South Asian regions, similar to the activity of another migrating noctuid pest, *Spodoptera litura*.<sup>24</sup>

Notably, non-native samples collected from South America were most similar to the Afro-Eurasian subgroup, with African samples showing the lowest level of genetic differentiation ( $F_{ST} = 0.005$ ). Pairwise  $d_{XY}$ <sup>25</sup> with *H. zea* showed that genetic divergence was lowest with South American *H. armigera*, consistent with evidence that *H. armigera* and *H. zea* hybridize in South America (Figure S5).<sup>23</sup> Combined, these results allow us to propose a preliminary scenario in which *H. armigera* began its spread from an ancestral origin in Africa before establishing on other continents. With more certainty, we can report that at least some invasive South American *H. armigera* were probably derived from African or European source populations.

### Local and global selective sweeps

*H. armigera* shows a broad geographic distribution that includes a variety of ecosystems, agricultural practices, and climates. To identify locally adapted alleles within each major lineage, we detected signatures of selective sweeps using a composite likelihood ratio (CLR) test.<sup>26,27</sup> We annotated a total of 1,805 genes within candidate-selected regions (Figure 2A). Most genes in selective sweep regions only showed signs of selection in one or a few lineages (Figure 2A), suggesting that the magnitude or efficacy of recent selection varies geographically. However, we found multiple candidate genes of interest (e.g., pesticide resistance-related genes: *CYP337B3*<sup>28,29</sup> and *AchE*<sup>30</sup>) that showed signs of consistent selection across lineages (Figure 2A; Table S7). The frequency of derived mutations within genes under selection and known to be associated with insecticide

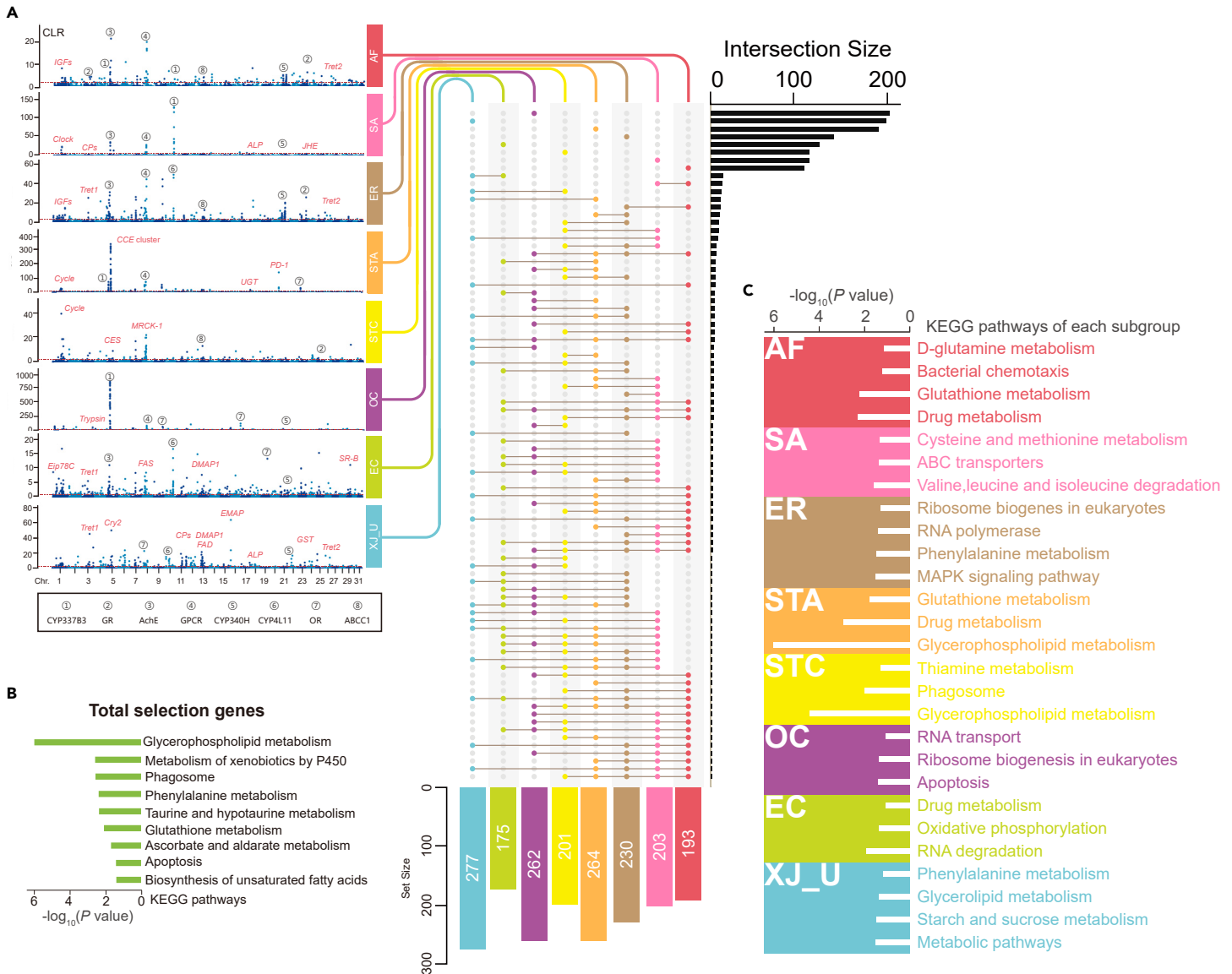


**Figure 2. Summary of genes under local adaptation for each subgroup** (A) Manhattan plots showing the detection of selection along the genome based on CLR values of each subgroup. The important candidate genes involved in environment adaptations are indicated in the Manhattan plots. The dashed lines indicate the top 1% threshold of CLR values. Shown is the distribution of genes in selective sweep regions in each lineage. Horizontal bars indicate the numbers of selected genes exclusively associated with one or multiple subgroups. Vertical bars represent genes under selection in each subgroup. (B and C) KEGG pathways identified as significantly overrepresented in overall selection regions and each subgroup ( $p < 0.05$ ).

resistance (*CYP337B3*, *AchE*, *GPCR*, and *CYP340H*) varied geographically (Figures S6–S9; Note S4). These results suggest that pesticide resistance spread rapidly either through gene flow over continent-scale distances or through convergent evolution. Some of the highest CLR values were seen in genes associated with pesticide resistance (e.g., *CYP337B3* in Oceania and the *CCE* cluster in South Asia; Figure 2A), implying that the most extreme and consistent selective pressures were anthropogenic. Kyoto Encyclopedia of Genes and Genomes (KEGG) functional enrichment analyses of individual genes in sweep regions revealed functional overrepresentation of lipid metabolism- and detoxification-related pathways. These included glycerophospholipid metabolism, metabolism of xenobiotics by P450s, and functions integral to the phagosome (Figure 2B). Genes under selection in Africa and East China were enriched in glutathione metabolism and drug metabolism, which may be due to the metabolism of pesticides or plant secondary metabolites. Selected genes from other lineages were enriched in diverse pathways, consistent with geographical differentiation of selected genes (Figure 2C). Genes associated with potentially non-anthropogenic selection pressures, such as those associated with host adaptation (*CYPs*, *GSTs*, and *UGTs*), olfactory reception (*OR* and *GR*), cold hardiness (*Tret1*, *Tret2*, and *FAS*), circadian rhythm (*clock*, *cycle*, and *Cry2*) and immunity (*Trypsin* and *SR-B*), were also observed (Figure 2A).

### Local adaptation to natural environments

Insects show complex adaptations to cold temperature, including diapause, a form of phenotypic plasticity in which development intermits, allowing individuals to avoid unfavorable conditions and synchronize their adult lifespan with optimal seasonal conditions.<sup>31</sup> Insect diapause often involves modification of body fluid composition to prevent ice crystal formation. The Xinjiang region is characterized by low winter temperatures (lower than  $-20^{\circ}\text{C}$ ) and seasonally variable day length, whereas temperatures rarely fall below  $20^{\circ}\text{C}$  in the tropical region of South China (Figure S10). *H. armigera* populations in these regions exhibit divergent adaptive traits, including photoperiod perception, diapause, and cold tolerance.<sup>12</sup> Under controlled conditions, *H. armigera* pupae derived from northern Chinese populations show heritable differences in the intensity and duration of diapause in response to light and temperature. Some tropical populations lack any diapause. This phenotypic plasticity is heritable and polygenic, although its exact genetic basis is unknown (Figure S11; Note S5).<sup>19,20</sup> To gain insight into the genetic basis of these adaptations, we searched for putative signals of selection by scanning the genome for high levels of genetic differentiation between these distinct lineages ( $F_{ST}$ ) and low levels of nucleotide diversity within populations ( $\pi$ ). Using the top fifth percentile of  $F_{ST}$  and  $\pi$  ratio, 302 candidate genes were identified within genomic regions under selection in Xinjiang (Figure S12;



Table S8). KEGG analysis showed that circadian rhythm, ABC transport, and several metabolism pathways were significantly enriched in this region (Figure S13). Genes associated with photoperiod perception (*CRY2*, *TIM*, *CLK*, and *CYC*) and long-wavelength opsin showed signatures of selection. These may be involved in adaptation to the highly variable diurnal rhythm in this region (Figure S12B), which seasonally varies between 10–16 h of sunlight in Xinjiang and 11–13 h of sunlight in South China. In addition to diapause, insects have many other strategies to mitigate exposure to low temperatures. These adaptations include behavioral avoidance to reduce the risk of freezing and loss of freezable water. Fatty acid and trehalose synthase genes were identified as putative targets of selection in the Xinjiang subgroup (Figure S12B). Their corresponding products, fatty acids and trehalose, are important cryoprotectants in diapause and cold tolerance. A cluster of ABCB transporter genes were also identified as targets of selection in Xinjiang. These genes have been associated with transport of amino acids, lipids, inorganic ions, and, especially, detoxification of xenobiotics. Within the South China subgroup, we identified 130 candidate genes within selected genomic regions (Figure S12B). KEGG analysis showed that the glutathione metabolism, amino acid biosynthesis, and oxidative phosphorylation pathways were significantly enriched (Figure S13). Signatures of selection at the chemosensory receptor, JH epoxide hydrolase, and the ionotropic glutamate receptor may reflect local adaptation to conditions in South China (e.g., high radiation, high humidity, and high host plant diversity; Table S9).

Diapause enables insects to cope with seasonal challenges such as extreme temperatures and a lack of suitable food. It provides a model for understanding adaptive evolution to natural environments.<sup>31,32</sup> We previously demonstrated that diapause-related traits are associated with latitude (Figure S11B; Note S5).<sup>12</sup> To explicitly investigate the genetic architecture underlying this adaptation in *H. armigera*, we performed a genome-wide environmental association study (enGWAS) incorporating a linear mixed model (LMM) for latitude among our samples (Table S10),<sup>33</sup> revealing six major-effect loci (Figure 3A). The strongest signal was identified on chromosome 1 in a 15-kb region containing the critical clock gene *cycle* (Figure 3B). In *Drosophila melanogaster*, *CYCLE* (*CYC*) and *CLOCK* (*CLK*) proteins heterodimerize and drive the transcription of *tim* and *per*, which are associated with diapause in *Ostrinia nubilalis*.<sup>34</sup> We found that *cycle* genotypes belong to three haplotypes (Figure 3C), which are geographically distributed from lowest- to highest-latitude regions. The second major-effect locus on chromosome 1 was the insulin-like growth factor (Figure 3D), which is also associated with diapause.<sup>35–37</sup> Similar to *cycle*, the genotypes of insulin-like also showed geographical distribution (Figure 3E). Trehalose transporter *Tret1* (chromosome 3 [chr3]) and the trehalose 6-phosphate synthase gene *TPS* (chr13) were also significantly associated with latitude (Figure 3A). Trehalose is the main blood sugar in insects, which is used as an energy source. Trehalose can also help protect against adverse environmental conditions, including low temperatures.<sup>38</sup> In addition to these loci, we observed a peak in chr6 in the intergenic region and a peak in chr12 containing the RYamide receptor-like gene; these require functional validation. The results suggest that diapause has evolved through several changes to a common temperature- and light-detecting pathway, as outlined in Figure 3F.

To study the genetic basis of cold tolerance, we performed an enGWAS using the minimum temperature of the coldest month (MTCM) and the mean temperature of the coldest quarter (MTCQ) (Figure S14; Table S10). Three loci associated with MTCM and four associated with MTCQ (Figure S14; enGWAS threshold,  $-\log p > 7.35$ ) were detected on chr3, chr6, and chr13 and on chr1, chr3, chr6, and chr13, respectively. The overlap between the associated loci among latitude and low temperature suggests that these two variables are correlated. Among these, the strongest signal was located on chr3, in which the highest-associated SNP (chr3: 6,628,922) was highly associated with MTCM ( $p = 5.02 \times 10^{-9}$ ) and MTCQ ( $p = 4.57 \times 10^{-9}$ ; Figures 4A and S14A). Using pairwise LD correlations, we identified *Tret1* within the association signal (chr3: 6,627,351–6,628,961). This gene contains one nonsynonymous SNP (chr3: 6,626,270), as confirmed through Sanger sequencing, which was significantly associated with MTCM and MTCQ (Figure S14B). In addition, selective sweep analysis between the Xinjiang and South China subgroups showed that the *Tret1* gene was positively selected for in Xinjiang (Figures S12B and S14C). Haplotype A (TAT, Ile) was overrepresented in samples from the cold Xinjiang region, whereas haplotype G (TGT, Thr) was mainly found in South China (Figure 4B). According to the global haplotype distribution (Figure 4B), we found

that haplotype A was locally adapted to extreme temperature variation within China and showed that data from China are better suited to test for adaptation. This SNP (c.1190G>A) is located in the fourth exon of *Tret1*, which encodes the amino acid substitution p.Thr397Ile (Figure 4C). *Tret1* was highly expressed in the pupa and fat body, which are suitable development stages and tissues to adapt to low temperatures (Figure S14D). Protein modeling with the Swiss model at greater than 90% accuracy showed that this Thr/Ile residue is located at the coupling helices (Figure 4D). The prediction of binding energies showed that the binding of haplotype A to trehalose is more stable (Figure S14E). We cloned and expressed the two haplotypes of *Tret1* in Hi5 cells and found that the Thr/Ile substitution did not affect its subcellular localization (Figure 4E) but significantly affected the transfer efficiency of trehalose (Figure 4F). Additionally, we isolated individuals from the two separated genotypes, *Tret*<sup>AA</sup> and *Tret*<sup>GG</sup>, in a single laboratory strain, thereby controlling for genetic background (Figure 4G), by genotyping using the nonsynonymous SNP (chr3: 6,626,270). After low-temperature treatment ( $-20^{\circ}\text{C}$ ), the concentration of trehalose in the pupae of group *Tret*<sup>AA</sup> was significantly higher than the concentration in group *Tret*<sup>GG</sup> (Figure 4H). In addition, supercooling point (SCP) results showed that the SCPs of group *Tret*<sup>AA</sup> were significantly lower than those of group *Tret*<sup>GG</sup> (Figure 4H;  $p < 0.01$ ). These results indicate that the derived *Tret1* haplotype A underlies a phenotype that enhances fitness in the cold Xinjiang region, where it is subject to positive selection. We found that the T397I mutation segregates in highly connected populations in relatively warm climates: South China (0.19% of individuals homozygous, 19.2% heterozygous) and South Asia (11% heterozygous). Whether this mutation spreads via gene flow into populations that occur in cold European climates and whether it will confer local adaptation and increase persistence in these regions remains unknown. Interestingly, *Tret1* was also found to be under selection in Europe (CLR,  $\sim 25$ ; Figure S15A). Although no nonsynonymous mutations were detected, *Tret1* haplotypes in Europe showed clear differences compared with those identified in East China and Xinjiang (Figure S15B), suggesting that *Tret1* may experience selection to cold climates in Asia and Europe.

The second major-effect SNP for cold tolerance was located on chr13 (2,719,321–2,720,127) and occurred in *TPS* (Figures S14A and S16A). Haplotypes at this locus showed frequency divergence between Xinjiang and South China (Figure S16B). Multi-amino acid substitutions in the conserved Glyco\_transf\_20 domain showed geographical structure (Figure S16C). The outlier region on chr3 containing *Tret1* and the peak on chr13 containing *TPS* were also confirmed using a latent factor mixed model (LFMM) (Figure S17). These results indicate that the synthesis and transport of trehalose may be involved in diapause and adaptation to low temperatures. The third major-effect locus in chr6 was located in the intergenic region, and its functions need further study (Figure S14A).

While temperature and latitude are highly correlated, the combined analyses allowed us to identify putative loci associated more significantly with one or both variables. Among the enGWAS results of latitude and low temperature (Figures 3A and S14A), we found three peaks associated with temperature and latitude on chr3 (*tret1*), chr6 (intergenic region), and chr13 (*TPS*). The adaptive ability to overwinter, requiring diapause and cryoprotectants, has likely arisen through several changes to a common temperature- and light-detecting pathway, as outlined in Figure 3F. This adaptation enables persistence of *H. armigera* at high latitudes.

### Local adaptation to anthropogenic environments

In addition to natural environmental factors, human activities such as insecticide applications can induce high selective pressures and result in rapid local adaptation.<sup>39</sup> The Xinjiang and North China lineages of *H. armigera* present an opportunity to identify adaptations to pesticide exposure. The two lineages are geographically and phylogenetically proximate, yet they experience different magnitudes of pesticide exposure. In contrast to the recently developed low-intensity agricultural practices in Xinjiang, agricultural activity in North China is highly developed. It occurs in concentrated sectors of arable land in a densely populated region with a long history of intensive pesticide use (see Note S1 and Figure S18A for further details).<sup>40,41</sup>

To characterize phenotypic divergence between populations in North China and Xinjiang, we performed insecticide sensitivity monitoring in the two regions in 2018–2019 (Figure 5A; Table S11). High levels of resistance to phoxim, cyhalothrin, and emamectin benzoate were observed in the North China population, including some populations with up to 216-fold resistance to cyhalothrin. By

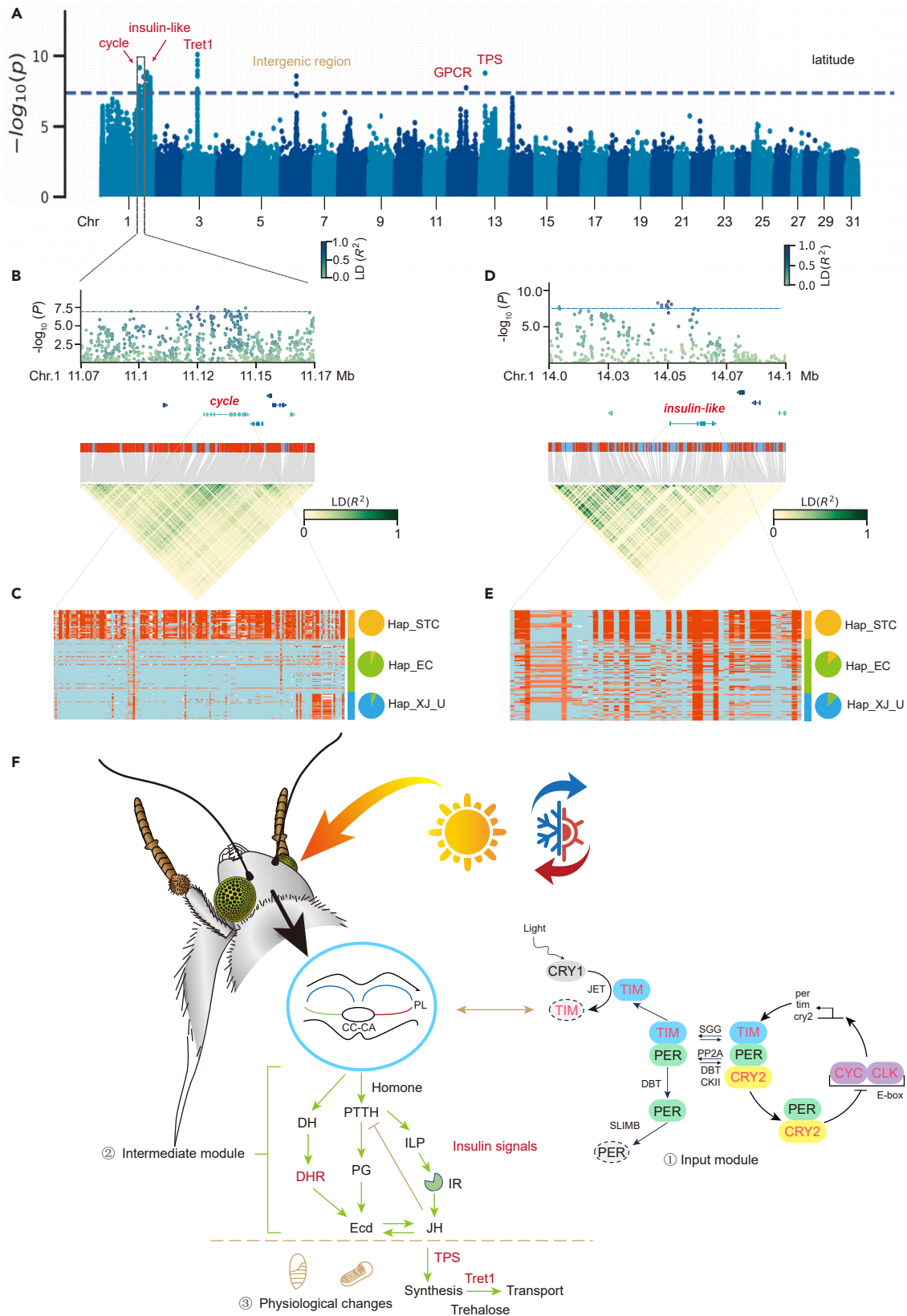


**Figure 3. Adaptive evolution of diapause** (A) enGWAS for latitude. Dashed lines indicate the significance threshold. (B) Local Manhattan plot, gene model, and local LD heatmap of the *cycle* gene region. (C) The haplotypes of the *cycle* gene in the three lineages. (D) Local Manhattan plot, gene model, and local LD heatmap of the *insulin-like* gene region. (E) The haplotypes of the *insulin-like* gene in three lineages. (F) Hypothesized mechanism of diapause adaptation. The light-sensing input module (1) consists of CLOCK (CLK) and CYCLE (CYC) heterodimers, which drive the transcription of *period* (*per*), *timeless* (*tim*), and *cryptochrome type 2* (*cry2*), whereby CRY2 is a negative regulator of CLK/CYC. CRY1 causes TIM degradation in a light-dependent manner to reset the phase of the clock. Through this upstream input module (labeled 1), light is detected, and the seasonally variable photoperiod is measured. Genes under positive selection in Xinjiang and those whose allelic variation was statistically associated with latitude are labeled in red. In the intermediate module (labeled 2), the circadian signaling pathway activates the release of hormones from the prothoracic gland (PG) because of stimulation of prothoracicotropic hormone (PTTH). PTTH and PG are associated with secretion of Ecd. The resulting physiological changes (labeled 3) include pupation and decreases in transcription, cellular respiration, and metabolism, allowing the pupa to conserve energy reserves and synthesize compounds such as trehalose.

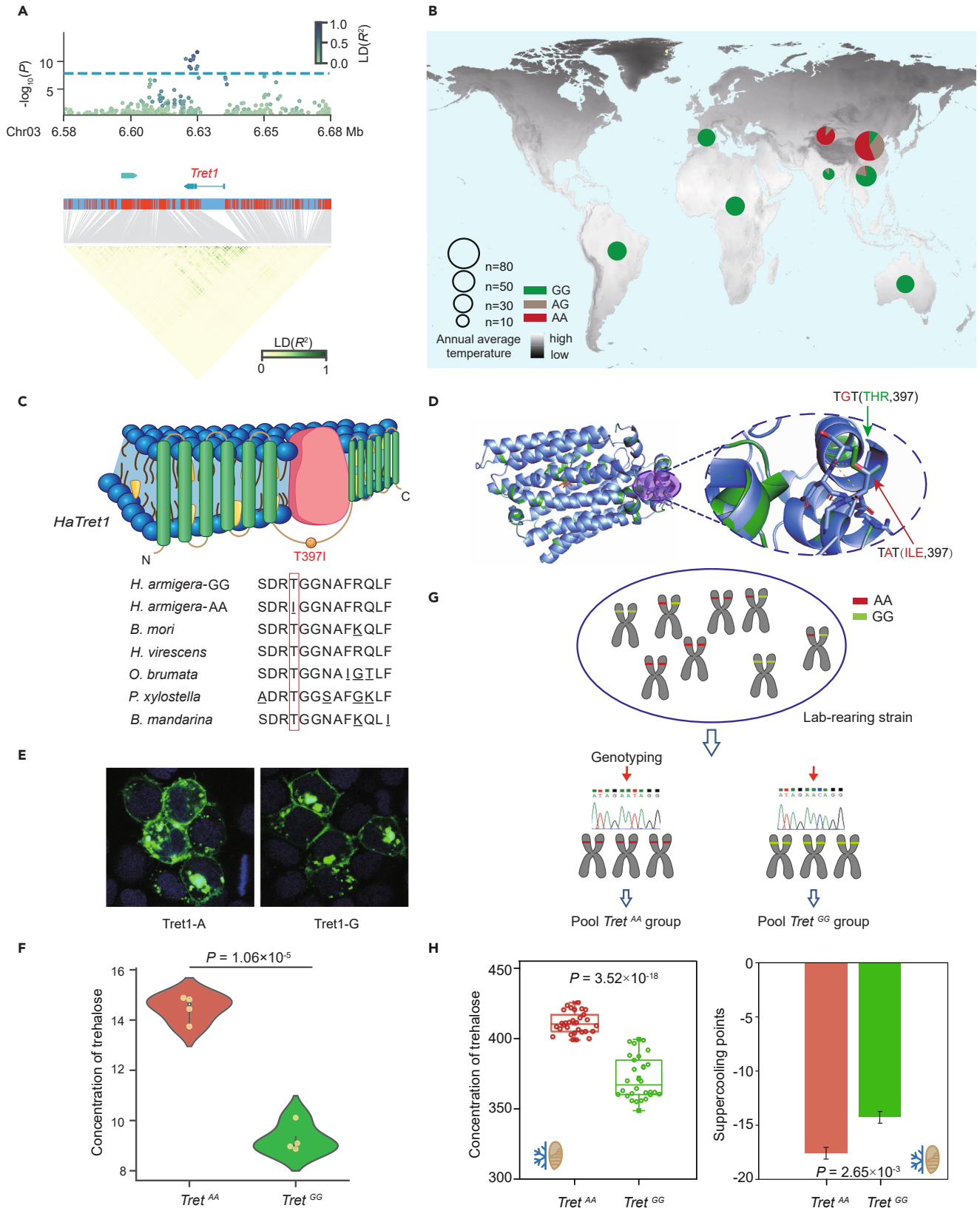


**Figure 4. Identification of *Tret1* associated with cold tolerance** (A) Association of *HaTret1* allelic variation with the MTCQ. The color key represents linkage disequilibrium values ( $r^2$ ). (B) Distribution of the frequency of *HaTret1* haplotypes among different geographical subgroups. (C) Multi-species alignment of the amino acid sequence of *HaTret1*. The amino acid substitution p.Thr397Ile is located in the intracellular region. (D) Protein structure modeling of *HaTret1*. The site for the p.Thr397Ile substitution is marked by arrows. (E) Localization of haplotypes A and G of *HaTret1* protein when expressed in Hi5 cells. (F) Trehalose transfer efficiency between haplotypes A and G in Hi5 cells ( $n = 4$  independent measurements; the  $p$  value was derived using Student's  $t$  tests). (G) Diagram of separated populations. After genotyping through the nonsynonymous SNP (chr3: 6626270), two separate groups, *Tret*<sup>AA</sup> and *Tret*<sup>GG</sup>, which possess similar genetic backgrounds, were obtained. (H) Left: measurement of trehalose concentrations in the pupae of two separate groups, *Tret*<sup>AA</sup> and *Tret*<sup>GG</sup>, after low-temperature treatment ( $-20^\circ\text{C}$ ). Right: the SCPs of two separate groups, *Tret*<sup>AA</sup> and *Tret*<sup>GG</sup>, were measured using 5-day-old pupae. Twenty pupae were used in the treatment, with three replicates.



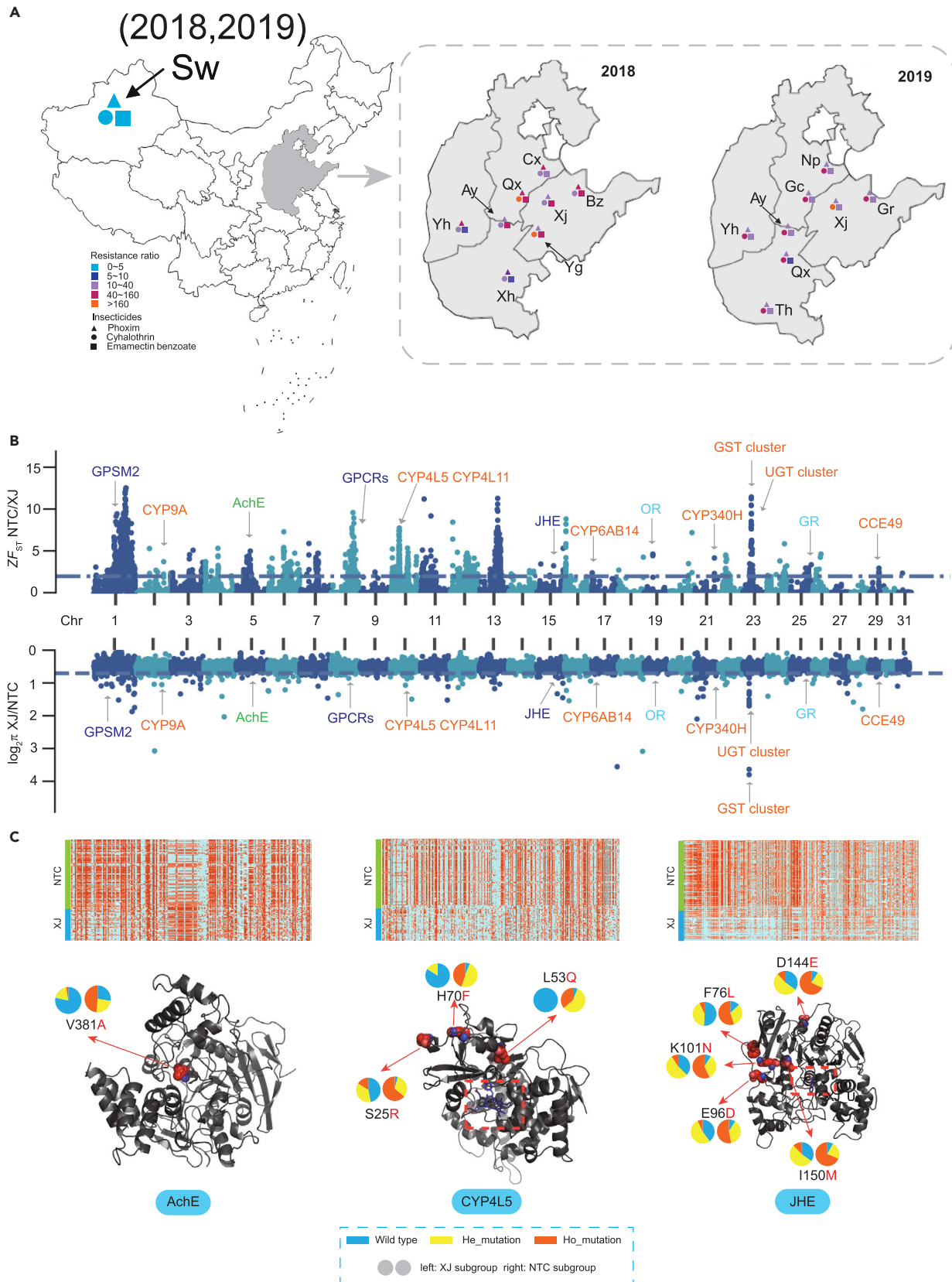


**Figure 5. Genetic basis of pesticide resistance** (A) Results of resistance monitoring of *H. armigera* to three insecticides in multi-sites of North China and Xinjiang in 2018–2019. Sampling regions in North China included Hebei, Henan, Shandong, and Shanxi provinces. Detailed information is listed in Table S10. (B) Genome-wide screening of insecticide selection signals, with  $ZF_{ST}$  (top) and  $\pi$  (bottom) comparing samples from North China and Xinjiang. Candidate genes known to be associated with insecticide resistance and occurring in outlier regions are labeled (red, detoxification enzymes; orange, signal transduction; green, pesticide target; blue, odorant and gustatory receptors). (C) Candidate genes *AchE*, *CYP4L5*, and *JHE* with strong selective sweep signals. Genotypes of SNPs in the above three genes (top). Protein structure model polymorphic sites labeled in *AchE*, *CYP4L5*, and *JHE*, which showed allelic variation between Xinjiang and North China (bottom). The frequency of homozygous wild types, homozygous derived variants (Ho\_mutation), and heterozygous sites (He\_mutation) are labeled for samples from Xinjiang (left) and North China (right).



contrast, populations in Xinjiang remain sensitive to these insecticides. This is likely due to a combination of regional differences in pesticide use and a lack of gene flow from North China populations (Figure S18A).

To identify potential mechanisms of rapid insecticide resistance evolution, we scanned the genome for extreme allele frequency divergence and nucleotide diversity between broadly resistant North China populations and susceptible Xinjiang populations (Figure 5B). Using the top fifth percentile of  $F_{ST}$  and  $\pi$  ratio, we identified 170 candidate genes falling within loci under selection in North China. Functional enrichment analysis showed that the CYP450 drug metabolism, glutathione metabolism, and oxidative phosphorylation pathways were enriched. This result is consistent with our expectation that this inter-population comparison would reveal signatures of selection on pesticide resistance loci. Cytochrome P450s in insects play a crucial role in resistance to synthetic insecticides and natural toxins and have been implicated in *H. armigera* pesticide resistance.<sup>42,43</sup> Outlier regions (Figure 5B) contained the CYP gene clusters CYP340 and CYP9A in addition to the genes *CYP4L5*, *CYP6AB20*, and *CYP4L11*, which all show geographic structure in the frequency of nonsynonymous alleles (Figure 5C; Table S12). A CYP9A gene cluster, which showed high similarity in protein sequences to the selected CYP9A gene cluster in this study, is associated with resistance to the insecticides abamectin and emamectin benzoate in the beet armyworm, *Spodoptera exigua* (Figures S18B and S18C).<sup>44</sup> Outlier regions also contained gene clusters associated with detoxification and pesticide resistance: glutathione S-transferases (six genes) and UDP-glucuronosyltransferases (six genes).<sup>45</sup> These detoxification genes are differentially expressed upon exposure to common pesticides<sup>46</sup> (Figure S18D). We found that the acetylcholinesterase (*AchE*) gene, which is an important target of carbamate and organophosphate insecticides,<sup>30</sup> was selected in North China (Figure 5B) and contained nine amino acid substitutions. The frequency of haplotype V318A in North China was significantly higher than that in Xinjiang (Figure 5C), consistent with positive selection imposed by insecticide usage in North China. Other outliers functionally associated with insecticide resistance included G-protein-signaling modulator 2, G-protein-coupled receptors, and juvenile hormone esterase (Figures 5C and S18B).<sup>47–49</sup> Finally, gustatory and olfactory receptors were identified as outliers, suggesting different chemical signal exposure in North China and Xinjiang.

A second difference in agricultural practice between Xinjiang and North China is exposure of *H. armigera* to Bt cotton. In North China, Bt cotton has been commercially grown since 1997 and currently constitutes almost 100% of all planted cotton. In contrast, the proportion of Bt cotton in Xinjiang has only recently increased and remains less than half that of North China (Figure S19). Monitoring data show that, after 2005, the Bt resistance level of cotton bollworm populations in North China gradually increased. By 2017, the resistance level had reached a low but significant level of 2- to 5-fold.<sup>50</sup> By contrast, Bt resistance in *H. armigera* populations in Xinjiang remains low. Contrary to expectations, the selective sweep analysis did not reveal candidate Bt receptor genes as outliers (Figure S20A). We also did not identify substitutions reported previously as resistant alleles in *CAD*,<sup>51</sup> *ABCC2*,<sup>52</sup> or *ABCC3*<sup>53</sup> (Figure S20B). However, the known *TSPAN* substitution L31S (Figure S20C), which is a dominant mutation,<sup>54</sup> was identified in North China (almost all carriers were heterozygous) and was absent in Xinjiang (Figure S20D). Thus, there is relatively little evidence for selection acting on known Bt resistance genes other than *TSPAN* L31S.

## DISCUSSION

Population genomics analyses are increasingly being used to infer species evolution, environmental adaptability and natural selection in mammal, plant, or model species<sup>4–7,55</sup> and are starting to be used to address formidable challenges caused by invasive insect pests. Clarifying the genetic basis of adaptive traits in crop pests and invasive species using population genomics is critical for understanding how these species establish and spread in new or extreme environments and for characterizing the major axes of population connectivity.<sup>56</sup> In the present study, we evaluated the functional diversity of *H. armigera* within its native range and demonstrated that population structure and genetic signatures of local and global adaptation are driven by climatic and anthropogenic selective forces. These findings shed light on the genetic architecture and biochemical basis of facultative diapause and cold tolerance, which are locally adapted and enable establishment of this pest in high-latitude environments. We also describe the geographic distribution of loci that are known to enable pesticide resistance.

Previous studies of the global population structure in *H. armigera* lacked either the geographic sampling breadth or the number of loci required to observe the subtle patterns of population structure that delimit the major lineages identified here.<sup>17,23</sup> The improved population phylogeny implies that *H. armigera* may have originated in Africa, spreading to Europe and South Asia and then to Oceania and East Asia. On a more recent timescale, our results suggest that invasive populations in South America were not derived from Oceania, East China, or Xinjiang but from the widely distributed and genetically diverse Afro-Eurasian lineage. Based on patterns of genetic differentiation, invasive South American individuals appear to be derived from an African or European source population. Samples from Africa and Europe show little genetic differentiation. Increased sampling in South America will be required to distinguish between single- and multi-source incursion events and to estimate source populations with greater precision. Our enhanced global sampling clarifies previous studies based on fewer genetic markers, which suggested a European origin of the South American invasion,<sup>57</sup> and research based on reduced-representation sequencing, pointing to an African and/or Asian source population.<sup>17</sup>

We also clarified the *H. armigera* population structure and genetic diversity throughout China. Samples from Xinjiang were highly distinct, with the reduced dispersal from this region reflecting biogeographic barriers to gene flow. These biogeographic barriers possibly prevent demographic swamping from other regions. Selection in Xinjiang has been sufficiently strong to enable local adaptation to the more extreme climatic conditions there. Mutations enhancing diapause and cold tolerance likely arose in Xinjiang because of selection pressures on shared pathways, underlying the circadian rhythm and trehalose synthesis and transport, linked by the genes *Tret1* and *TPS*. By this mechanism, a species that thrives in the tropics can successfully overwinter in regions where winter temperatures can drop below  $-20^{\circ}\text{C}$ .

*H. armigera* can migrate long distances and thereby introduce resistance alleles into new populations (including potentially North America; Figure S21) and even related species. This poses a significant threat to new habitats and existing populations.<sup>58,59</sup> This is reflected in the generally low population differentiation that occurs at a global scale. Therefore, fitness-enhancing mutations—especially those with a simple genetic basis, including many pesticide resistance alleles—can readily spread across continents. This may explain the set of known pesticide resistance genes that show signs of selection across multiple *H. armigera* lineages (Figure 2; Note S6). We also found clear signatures of positive selection on insecticide receptors and metabolic enzymes in a highly connected East Chinese population, implying that these adaptive CYP mutations could spread to other *H. armigera* populations. These results highlight the need to stem anthropogenic *H. armigera* dispersal, especially via southern Asia, to limit the spread of resistance alleles, such as those affecting Bt efficacy, which threatens global food security. Our analysis of anthropogenic selection suggests that *H. armigera* management strategies must be integrated globally and multilaterally because agricultural practices that enhance pesticide resistance even in relatively isolated regions can affect agriculture at a global scale.

## MATERIALS AND METHODS

See supplemental information for details.

## REFERENCES

- Bradshaw, C.J.A., Leroy, B., Bellard, C., et al. (2016). Massive yet grossly underestimated global costs of invasive insects. *Nat. Commun.* **7**, 12986.
- Early, R., Bradley, B.A., Dukes, J.S., et al. (2016). Global threats from invasive alien species in the twenty-first century and national response capacities. *Nat. Commun.* **7**, 12485.
- Bock, D.G., Caseys, C., Cousens, R.D., et al. (2015). What we still don't know about invasion genetics. *Mol. Ecol.* **24**, 2277–2297.
- Gu, Z., Pan, S., Lin, Z., et al. (2021). Climate-driven flyway changes and memory-based long-distance migration. *Nature* **591**, 259–264.
- Lovell, J.T., MacQueen, A.H., Mamidi, S., et al. (2021). Genomic mechanisms of climate adaptation in polyploid bioenergy switchgrass. *Nature* **590**, 438–444.
- Orteu, A., and Jiggins, C.D. (2020). The genomics of coloration provides insights into adaptive evolution. *Nat. Rev. Genet.* **21**, 503.
- Sinding, M.H.S., Gopalakrishnan, S., Ramos-Madrugal, J., et al. (2020). Arctic-adapted dogs emerged at the Pleistocene-Holocene transition. *Science* **368**, 1495–1499.
- Bertelsmeier, C., and Keller, L. (2018). Bridgehead effects and role of adaptive evolution in invasive populations. *Trends Ecol. Evol.* **33**, 527–534.
- Tay, W.T., and Gordon, K.H.J. (2019). Going global - genomic insights into insect invasions. *Curr. Opin. Insect Sci.* **31**, 123–130.

10. Kriticos, D.J., Ota, N., Hutchison, W.D., et al. (2015). The potential distribution of invading *Helicoverpa armigera* in North America: is it just a matter of time? *PLoS One* **10**, e0133224.
11. Jones, C.M., Parry, H., Tay, W.T., et al. (2019). Movement ecology of pest *Helicoverpa*: implications for ongoing spread. *Annu. Rev. Entomol.* **64**, 277–295.
12. Wu, K.M., and Guo, Y.Y. (2005). The evolution of cotton pest management practices in China. *Annu. Rev. Entomol.* **50**, 31–52.
13. Liu, Z., Gong, P., Li, D., et al. (2010). Pupal diapause of *Helicoverpa armigera* (Hübner) (Lepidoptera: Noctuidae) mediated by larval host plants: pupal weight is important. *J. Insect Physiol.* **56**, 1863–1870.
14. Jones, C.M., Papanicolaou, A., Mironidis, G.K., et al. (2015). Genomewide transcriptional signatures of migratory flight activity in a globally invasive insect pest. *Mol. Ecol.* **24**, 4901–4911.
15. Wilson, L.J., Whitehouse, M.E.A., and Herron, G.A. (2018). The management of insect pests in Australian cotton: an evolving story. *Annu. Rev. Entomol.* **63**, 215–237.
16. Xiao, Y., Li, W., Yang, X., et al. (2021). Rapid spread of a densovirus in a major crop pest following wide-scale adoption of Bt-cotton in China. *Elife* **10**, e66913.
17. Anderson, C.J., Tay, W.T., Mcgaughan, A., et al. (2016). Population structure and gene flow in the global pest, *Helicoverpa armigera*. *Mol. Ecol.* **25**, 5296–5311.
18. Behere, G.T., Tay, W.T., Russell, D.A., et al. (2013). Population genetic structure of the cotton bollworm *Helicoverpa armigera* (Hubner) (Lepidoptera: Noctuidae) in India as inferred from EPIC-PCR DNA markers. *PLoS One* **8**, e53448.
19. Chen, Y.S., Chen, C., He, H.M., et al. (2013). Geographic variation in diapause induction and termination of the cotton bollworm, *Helicoverpa armigera* Hubner (Lepidoptera: Noctuidae). *J. Insect Physiol.* **59**, 855–862.
20. Chen, C., Xia, Q.W., Chen, Y.S., et al. (2012). Inheritance of photoperiodic control of pupal diapause in the cotton bollworm, *Helicoverpa armigera* (Hubner). *J. Insect Physiol.* **58**, 1582–1588.
21. Sheng, Y., and Song, L. (2019). Agricultural production and food consumption in China: a long-term projection. *China Econ. Rev.* **53**, 15–29.
22. Pearce, S.L., Clarke, D.F., East, P.D., et al. (2017). Genomic innovations, transcriptional plasticity and gene loss underlying the evolution and divergence of two highly polyphagous and invasive *Helicoverpa* pest species. *BMC Biol.* **15**, 63.
23. Anderson, C.J., Oakeshott, J.G., Tay, W.T., et al. (2018). Hybridization and gene flow in the mega-pest lineage of moth, *Helicoverpa*. *Proc. Natl. Acad. Sci. USA* **115**, 5034–5039.
24. Cheng, T., Wu, J., Wu, Y., et al. (2017). Genomic adaptation to polyphagy and insecticides in a major East Asian noctuid pest. *Nat. Ecol. Evol.* **1**, 1747–1756.
25. You, M., Ke, F., You, S., et al. (2020). Variation among 532 genomes unveils the origin and evolutionary history of a global insect herbivore. *Nat. Commun.* **11**, 2321.
26. Ji, Y., Li, X., Ji, T., et al. (2020). Gene reuse facilitates rapid radiation and independent adaptation to diverse habitats in the Asian honeybee. *Sci. Adv.* **6**, eabd3590.
27. Pavlidis, P., Živkovic, D., Stamatakis, A., et al. (2013). SweeD: likelihood-based detection of selective sweeps in thousands of genomes. *Mol. Biol. Evol.* **30**, 2224–2234.
28. Joußen, N., Agnolet, S., Lorenz, S., et al. (2012). Resistance of Australian *Helicoverpa armigera* to fenvalerate is due to the chimeric P450 enzyme CYP337B3. *Proc. Natl. Acad. Sci. USA* **109**, 15206–15211.
29. Rasool, A., Joußen, N., Lorenz, S., et al. (2014). An independent occurrence of the chimeric P450 enzyme CYP337B3 of *Helicoverpa armigera* confers cypermethrin resistance in Pakistan. *Insect Biochem. Molec.* **53**, 54–65.
30. Fulton, M.H., and Key, P.B. (2001). Acetylcholinesterase inhibition in estuarine fish and invertebrates as an indicator of organophosphorus insecticide exposure and effects. *Environ. Toxicol. Chem.* **20**, 37–45.
31. Ragland, G.J., Armbruster, P.A., and Meuti, M.E. (2019). Evolutionary and functional genetics of insect diapause: a call for greater integration. *Curr. Opin. Insect Sci.* **36**, 74–81.
32. Xu, W.H., Lu, Y.X., and Denlinger, D.L. (2012). Cross-talk between the fat body and brain regulates insect developmental arrest. *Proc. Natl. Acad. Sci. USA* **109**, 14687–14692.
33. Lasky, J.R., Upadhyaya, H.D., Ramu, P., et al. (2015). Genome-environment associations in sorghum landraces predict adaptive traits. *Sci. Adv.* **1**, e1400218.
34. Kozak, G.M., Wadsworth, C.B., Kahne, S.C., et al. (2019). Genomic basis of circannual rhythm in the European corn borer moth. *Curr. Biol.* **29**, 3501–3509.e5.
35. Williams, K.D., Busto, M., Suster, M.L., et al. (2006). Natural variation in *Drosophila melanogaster* diapause due to the insulin-regulated PI3-kinase. *Proc. Natl. Acad. Sci. USA* **103**, 15911–15915.
36. Zhang, X.S., Wang, T., Lin, X.W., et al. (2017). Reactive oxygen species extend insect life span using components of the insulin-signaling pathway. *Proc. Natl. Acad. Sci. USA* **114**, E7832–E7840.
37. Li, H.Y., Wang, T., Yang, Y.P., et al. (2017). TGF-beta signaling regulates p-Akt levels via PP2A during diapause entry in the cotton bollworm, *Helicoverpa armigera*. *Insect Biochem. Molec.* **87**, 165–173.
38. Kanamori, Y., Saito, A., Hagiwara-Komoda, Y., et al. (2010). The trehalose transporter 1 gene sequence is conserved in insects and encodes proteins with different kinetic properties involved in trehalose import into peripheral tissues. *Insect Biochem. Molec.* **40**, 30–37.
39. Walsh, T.K., Heckel, D.G., Wu, Y., et al. (2022). Determinants of insecticide resistance evolution: comparative analysis among *Heliothines*. *Annu. Rev. Entomol.* **67**, 387–406.
40. Wang, G., and Fok, M. (2018). Managing pests after 15 years of Bt cotton: farmers' practices, performance and opinions in northern China. *Crop Prot.* **110**, 251–260.
41. Wang, Z.G., Jiang, S.S., Mota-Sanchez, D., et al. (2019). Cytochrome P450-mediated lambda-delta-cyhalothrin-resistance in a field strain of *Helicoverpa armigera* from Northeast China. *J. Agric. Food Chem.* **67**, 3546–3553.
42. Wang, H., Shi, Y., Wang, L., et al. (2018). CYP6AE gene cluster knockout in *Helicoverpa armigera* reveals role in detoxification of phytochemicals and insecticides. *Nat. Commun.* **9**, 4820.
43. Durigan, M.R., Corrêa, A.S., Pereira, R.M., et al. (2017). High frequency of CYP337B3 gene associated with control failures of *Helicoverpa armigera* with pyrethroid insecticides in Brazil. *Pestic. Biochem. Physiol.* **143**, 73–80.
44. Zuo, Y., Shi, Y., Zhang, F., et al. (2021). Genome mapping coupled with CRISPR gene editing reveals a P450 gene confers avermectin resistance in the beet armyworm. *PLoS Genet.* **17**, e1009680.
45. Li, X., Schuler, M.A., and Berenbaum, M.R. (2007). Molecular mechanisms of metabolic resistance to synthetic and natural xenobiotics. *Annu. Rev. Entomol.* **52**, 231–253.
46. Jin, M., Liao, C., Chakrabarty, S., et al. (2019). Transcriptional response of ATP-binding cassette (ABC) transporters to insecticides in the cotton bollworm, *Helicoverpa armigera*. *Pestic. Biochem. Physiol.* **154**, 46–59.
47. Li, T., Liu, L., Zhang, L., et al. (2014). Role of G-protein-coupled receptor-related genes in insecticide resistance of the mosquito, *Culex quinquefasciatus*. *Sci. Rep.* **4**, 6474.
48. Liu, N., Wang, Y., Li, T., et al. (2021). G-protein coupled receptors (GPCRs): signaling pathways, characterization, and functions in insect physiology and toxicology. *Int. J. Mol. Sci.* **22**, 5260.
49. Taylor, M.F.J., Park, Y., and Shen, Y. (1996). Molecular population genetics of sodium channel and juvenile hormone esterase markers in relation to pyrethroid resistance in *Heliothis virescens* (Lepidoptera: Noctuidae). *Ann. Entomol. Soc. Am.* **89**, 728–738.
50. Dandan, Z., Yutao, X., Wenbo, C., et al. (2019). Field monitoring of *Helicoverpa armigera* (Lepidoptera: Noctuidae) Cry1Ac insecticidal protein resistance in China (2005–2017). *Pest Manag. Sci.* **75**, 753–759.
51. Zhang, H., Tian, W., Zhao, J., et al. (2012). Diverse genetic basis of field-evolved resistance to Bt cotton in cotton bollworm from China. *Proc. Natl. Acad. Sci. USA* **109**, 10275–10280.
52. Gahan, L.J., Pauchet, Y., Vogel, H., et al. (2010). An ABC transporter mutation is correlated with insect resistance to *Bacillus thuringiensis* Cry1Ac toxin. *PLoS Genet.* **6**, e1001248.
53. Chen, Z., He, F., Xiao, Y., et al. (2015). Endogenous expression of a Bt toxin receptor in the Cry1Ac-susceptible insect cell line and its synergistic effect with *cadherin* on cytotoxicity of activated Cry1Ac. *Insect Biochem. Molec.* **59**, 1–17.
54. Jin, L., Wang, J., Guan, F., et al. (2018). Dominant point mutation in a tetraspanin gene associated with field-evolved resistance of cotton bollworm to transgenic Bt cotton. *Proc. Natl. Acad. Sci. USA* **115**, 11760–11765.
55. Therkildsen, N.O., Wilder, A.P., Conover, D.O., et al. (2019). Contrasting genomic shifts underlie parallel phenotypic evolution in response to fishing. *Science* **365**, 487–490.
56. Wu, N., Zhang, S., Li, X., et al. (2019). Fall webworm genomes yield insights into rapid adaptation of invasive species. *Nat. Ecol. Evol.* **3**, 105–115.
57. Gonçalves, R.M., Mastrangelo, T., Rodrigues, J.C.V., et al. (2019). Invasion origin, rapid population expansion, and the lack of genetic structure of cotton bollworm (*Helicoverpa armigera*) in the Americas. *Ecol. Evol.* **9**, 7378–7401.
58. Valencia-Montoya, W.A., Elfekih, S., North, H.L., et al. (2020). Adaptive introgression across semipermeable species boundaries between local *Helicoverpa zea* and invasive *Helicoverpa armigera* moths. *Mol. Biol. Evol.* **37**, 2568–2583.
59. Walsh, T.K., Joussem, N., Tian, K., et al. (2018). Multiple recombination events between two cytochrome P450 loci contribute to global pyrethroid resistance in *Helicoverpa armigera*. *PLoS One* **13**, e0197760.

## ACKNOWLEDGMENTS

We thank Shuai Zhang in the Ministry of Agriculture and Rural Affairs of the People's Republic of China and Wei Fan and Yuxiao Chang in the Agricultural Genomics Institute at Shenzhen, Chinese Academy of Agricultural Sciences for comments. We thank Yanhui Lu and Bing Liu in the Plant Protection Institute of the Chinese Academy of Agricultural Science for help with sample collection. This project was funded by the Agricultural Science and Technology Innovation Program of the Chinese Academy of Agricultural Sciences and Major Projects of Basic Research of Science, The Sci-Tech Innovation 2030 Agenda (2022ZD04021), the Technology and Innovation Commission of Shenzhen Municipality, the United Kingdom's Biotechnology and Biological Sciences Research Council (BB/L026821/1), and Research Councils UK (BB/P023444/1) (to K.W.). C.J. and H.L.N. were funded by BBSRC (BB/G105364/1). H.L.N. was supported by the University of Cambridge Department of Zoology. S.E. was funded by EMBO fellowship ATSF-6889 and the CSIRO-Julius Award (R-91040-11). W.A.V.M. was supported by the Lemann Brazil Research Fund from Harvard University.

## AUTHOR CONTRIBUTIONS

Y.X., K.W., and C.J. conceived and designed the study. M.J., W.A.V.M., T.T., and Yan Zhou collected samples. H.L.N. and C.J. advised and collaborated on population genomics analysis. M.J., Y.P., H.L., B.L., R.P., and W.Z. analyzed the data. S.E. and T.W. obtained sequence data from outside of China. H.L.N. performed data filtering and quality control for samples collected outside of China. M.J., S.E., and K.L. conducted the experiments. M.J. and Y.X. wrote the manuscript along with H.L.N. with input from all authors.

**DECLARATION OF INTERESTS**

The authors declare no competing interests.

**DATA AND CODE AVAILABILITY**

All sequencing data generated in this project are available at NCBI under BioProjects SAMN18253696 (genome) and PRJNA713413 (re-sequencing).

**SUPPLEMENTAL INFORMATION**

It can be found online at <https://doi.org/10.1016/j.xinn.2023.100454>.

**LEAD CONTACT WEBSITE**

<https://agis.caas.cn/kydw/kydwyjzx/stjzyjzx/a60d88a084114026bbe51b23e5a5cc59.htm>.